

Article

Growth and Characterization of Second and Third Order Acentric Studies of L-Phenylalanine L-Phenylalaninium Malonate Single Crystal

P. Sangeetha ¹, M. Nageshwari ², C. Rathika Thaya Kumari ², S. Srividhya ³, G. Vinitha ⁴, G. Mathubala ⁵, A. Manikandan ⁵ , M. Lydia Caroline ⁶, Anish Khan ^{7,8,*} , Hajer S. Alorfi ⁸, Mahmoud Ali Hussein ^{8,9}  and Madhu Puttegowda ^{7,8}

- ¹ PG & Research, Department of Physics, Arignar Anna Government Arts College, Cheyyar 604407, Tamil Nadu, India; sangeepaari@gmail.com
- ² Department of Physics, Bharath Institute of Higher Education and Research, Chennai 600073, Tamil Nadu, India; nageshwari.sb@gmail.com (M.N.); rathikak06@gmail.com (C.R.T.K.)
- ³ Department of Physics, Indian Maritime University, Uthandi, Chennai 600119, Tamil Nadu, India; srividya@imu.ac.in
- ⁴ Department of Physics, School of Advanced Sciences, VIT, Chennai 600127, Tamil Nadu, India; vinitha.g@vit.ac.in
- ⁵ Department of Chemistry, Bharath Institute of Higher Education and Research, Chennai 600073, Tamil Nadu, India; mathubala.che@bharathuniv.ac.in (G.M.); manikandana.che@bharathuniv.ac.in (A.M.)
- ⁶ Department of Physics, Dr. Ambedkar Govt. Arts College, Vyasarpadi, Chennai 600039, Tamil Nadu, India; lydiacaroline2013@gmail.com
- ⁷ Center of Excellence for Advanced Materials Research, King Abdulaziz University, P.O. Box 80203, Jeddah 21589, Saudi Arabia; madhu.p.gowda15@gmail.com
- ⁸ Chemistry Department, Faculty of Science, King Abdulaziz University, P.O. Box 80203, Jeddah 21589, Saudi Arabia; hsalorfi@gmail.com (H.S.A.); mahusseini74@yahoo.com (M.A.H.)
- ⁹ Chemistry Department, Faculty of Science, Assiut University, Assiut 71516, Egypt
- * Correspondence: anishkhan97@gmail.com



Citation: Sangeetha, P.; Nageshwari, M.; Kumari, C.R.T.; Srividhya, S.; Vinitha, G.; Mathubala, G.; Manikandan, A.; Caroline, M.L.; Khan, A.; Alorfi, H.S.; et al. Growth and Characterization of Second and Third Order Acentric Studies of L-Phenylalanine L-Phenylalaninium Malonate Single Crystal. *Crystals* **2022**, *12*, 869. <https://doi.org/10.3390/cryst12060869>

Academic Editors: Drialys Car-denas-Morcoso, Hung-Pin Hsu and Franziska Simone Hegner

Received: 5 April 2022
Accepted: 13 June 2022
Published: 20 June 2022

Publisher's Note: MDPI stays neutral with regard to jurisdictional claims in published maps and institutional affiliations.



Copyright: © 2022 by the authors. Licensee MDPI, Basel, Switzerland. This article is an open access article distributed under the terms and conditions of the Creative Commons Attribution (CC BY) license (<https://creativecommons.org/licenses/by/4.0/>).

Abstract: A single crystal of L-phenylalanine L-phenylalaninium malonate (LPPMA) was synthesized by slow evaporation and was subjected to nonlinear optical examination and physio-chemical characterization. Studies on single X-ray diffraction confirm the arrangement of monoclinic space group P21 which is a vital criterion for the NLO phenomenon. The assessment of functional groups and diverse vibration modes responsible for the characteristics of the material was performed with an FTIR analysis. The UV-visible spectral examination found the wavelength of UV-cutoff at 233 nm and various optical parameters were evaluated. The mechanical strength and different criteria associated with it were assessed. The electric field response of the material was examined in terms of the dielectric constant, dielectric loss, ac conductivity and activation energy. The spectra of emission were detailed. The efficacy of second harmonic generation was studied. The parameters of non-linearity were investigated to analyse the third-order acentric optical response in the LPPMA by Z-scan procedure.

Keywords: nonlinear optics; activation energy; fluorescence; SHG; Z-scan method

1. Introduction

Materials exhibiting second (SHG), third (THG) and higher harmonic generation occupy a versatile position in the area of optical data storage with information processing. The photo-electric interface occurs in the process of nonlinear SHG, and finds promising potential in the domain of storage of data with high intensity and spectroscopy [1]. The significance of the basic types with their orientations inside the material plays a substantial part in finding or understanding the physical and chemical features of the organic

molecules in a material. For a material to possess nonlinear optical characteristics, molecular dipoles align in a noncentric fashion, which is indispensable for materials with an SHG property [2]. A greater number of organic compounds materialize in the space group of Centro symmetry and do not have a nonlinear optical feature. To remedy this, various molecular engineering approaches such as steric-hindrance, chirality, etc., have been proposed [2]. The main aspect of amino acids in the nonlinear optical domain mainly solidifies in noncentrosymmetric space groups. In the organic category, α - amino acids have distinct characteristics [3]. Crystals grown from amino acids possess fascinating features suitable for NLO devices, because of their zwitterionic nature which initiates the hydrogen bonding network [4]. Among nonlinear optical materials, organic materials act as a midway between compounds of the organic category with covalent bonds and inorganic compounds with mostly ionic bonds [5]. The production of organic acentric crystals exposes the poor stability of their physico-chemical features and their lower mechanical strength. Amino acid-based crystals, with their outstanding electro-optic and NLO properties, show abundant response in photonic applications [6,7]. Currently, organic molecules with third-order nonlinearity are essential for widespread applications in 3D optical memory and optical communication with information processing at high speeds [8]. Relatedly, L-phenylalanine-based complex materials [9–13] prove to be more prospective materials for NLO applications. Reasonably, some authors have shown interest in working with malonic acid-based crystals and report it as an effective NLO material [14–16] suitable for optical applications. Furthermore, the structure and certain studies of LPPMA were reported by Alagar and Prakash [17,18]. Here, we studied the growth and characterization of LPPMA samples using the slow evaporation process. LPPMA crystals were characterized using various instrumentation systems to check their suitability for device fabrications.

2. Experimental

Synthesis of LPPMA

L-phenylalanine L-phenylalaninium malonate (LPPMA) was produced using slow solvent solution growth (evaporation), SSEST with deionized water, which was harvested from the starting compound L-phenylalanine (LOBA, 99%), and malonic acid (LOBA, 99%) in stoichiometric molar (2:1). The estimated quantity of materials was systematically dissolved in water. The mixture was stirred continuously using a magnetic stirrer for 6 h to ensure complete miscibility. The well saturated and filtered solution was transferred into a 250 ml beaker, covered with filter paper containing tiny pin-holes and set aside at room temperature. Colorless transparent crystals were observed in 25 days and harvested (Figure 1).



Figure 1. The photograph of LPPMA.

3. Discussion of Results

3.1. X-ray Diffraction (Single Crystal)

The result of the XRD showed that LPPMA crystallizes in a monoclinic arrangement. The lattice parameters revealed in the SXRD investigation are provided in Table 1, which shows the agreement between our results and those reported in the literature [18].

Table 1. The crystallographic data (SXRD) of LPPMA.

Lattice Parameter	Present Work	Reported Work [18]
Space group	P2 ₁	P2 ₁
a (Å)	14.16	14.02
b (Å)	5.56	5.507
c (Å)	14.74	14.59
β (°)	107.28	107.39
Volume (Å ³)	1108	1075.2

3.2. FTIR Vibrational Analyses

The data regarding the structure of a material are evident from this spectroscopic analysis. The absorption of IR radiation leads to diverse peaks in a particle, showing stretching and bending vibration as represented in Figure 2. A strong broad absorption in the range of 3300–2300 cm⁻¹ agrees with the NH₃⁺ of the amino group [18]. The strong edge at 3081 cm⁻¹ is C-H stretching. Overtone combination appears in the absorption region at 2090 cm⁻¹. The peaks at 1302, 1359 cm⁻¹ exhibit CH₂ wagging and CH₂ deformation [19,20]. The wavenumber positioned at 1210 cm⁻¹ is C-CH in a sharp bending vibration. C-C and C-N stretching are identifiable in wavenumbers 1140, 1183 cm⁻¹ [18]. The vibration of C-H out of plane (bending) initiates peaks at 953 and 914 cm⁻¹. The wavenumber at 701 cm⁻¹ exhibits the presence of a benzene ring. Thus, peaks which appear at 853 cm⁻¹, 748 cm⁻¹ establish C-H (out of) plane deformation [17].

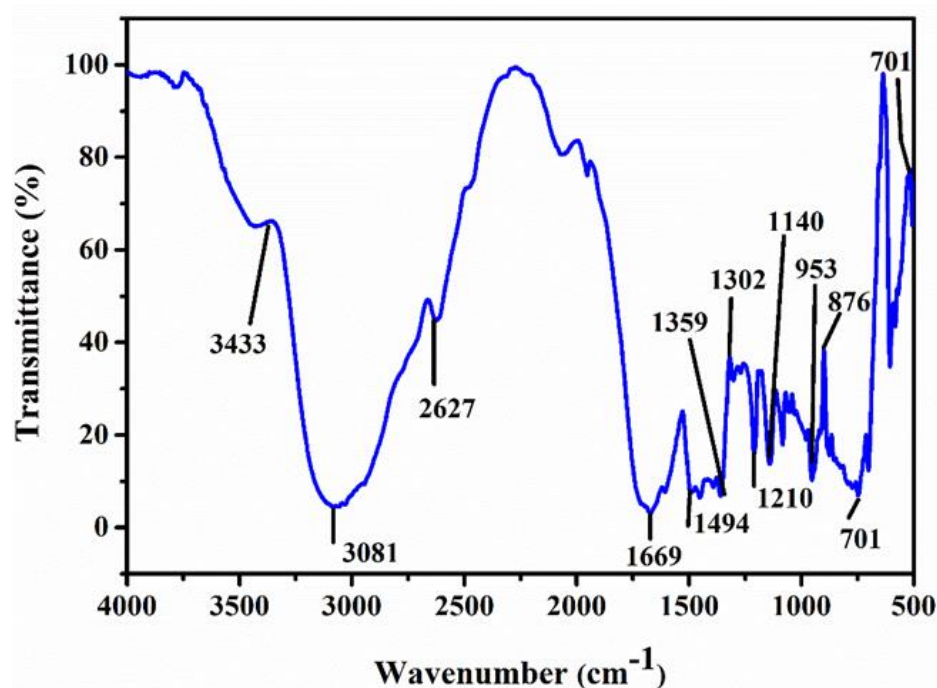


Figure 2. FTIR profile of LPPMA.

3.3. Optical Studies

The optical spectrum of LPPMA was established in the 200–700 nm wavelength range. From the UV-visible spectrum (Figure 3a), it is clear that ultraviolet absorption includes electronic transitions from an unexcited state to an excited one [21]. The lower cutoff wavelength of LPPMA at 233 nm with extremely good transparency proves its applicability in second and third harmonic generation. The absorption coefficient (α) was assessed utilizing the following Formula

$$\alpha = \frac{2.3026 \log(1/T)}{d} \tag{1}$$

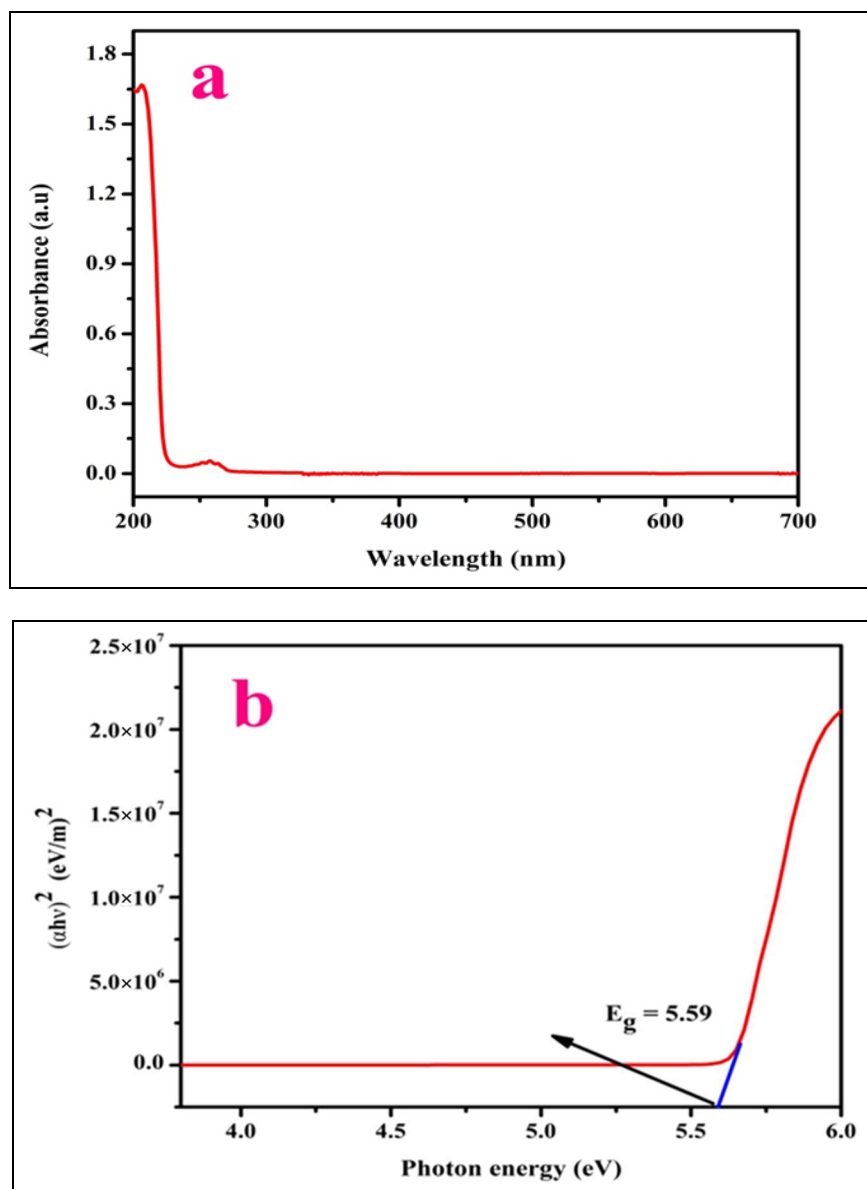


Figure 3. (a) Profile of optical spectrum and (b) Tauc’s graph of LPPMA.

Here, d represents material thickness. The absorption coefficient represented as (α) was evaluated using Tauc’s concept:

$$\alpha = A \frac{(h\nu - E_g)^2}{h\nu} \tag{2}$$

where A symbolizes the constant and E_g , h and v represent the energy gap, the value of the Planck constant (6.63×10^{-34} Jsec), and frequency of photons. The energy gap E_g of LPPMA was estimated using Tauc's plot (Figure 3b) and its value is 5.58 eV. Thus, the organic LPPMA crystal with an enhanced optical band gap is a potential aspirant in the field of nonlinear optics.

3.3.1. Optical Constants Calculation

The optical nature of a material is very important in determining its usefulness in NLO application devices. The diverse optical constants were evaluated utilizing the subsequent formulae [21]. Extinction coefficient (K) can be estimated by

$$K = \frac{\lambda\alpha}{4\pi} \quad (3)$$

Reflectance (R) and linear refractive index (n_0) are assessed using [4]

$$R = 1 \pm \frac{\sqrt{1 - \exp(-\alpha t) + \exp(\alpha t)}}{1 + \exp(-\alpha t)} \quad (4)$$

$$n_0 = - \left\{ \frac{(R + 1) \pm \sqrt{3R^2 - 10R - 3}}{2(R - 1)} \right\} \quad (5)$$

Figure 4a,b, depict that R and K fully rely on incident photon energy [21]. Figure 4c,d depicts (R) and (K) versus the absorption coefficient (α). The device internal efficacy mainly relies on this absorption coefficient (α) [21]. Figure 4e displays the dependence of linear n_0 (refractive index) versus incident energy (photon). The minimum value of n_0 highlights that LPPMA has a regular dispersion nature. The high optical transparency of LPPMA in the Ultraviolet-visible section illustrates it as a good optical behavior candidate for use in device applications.

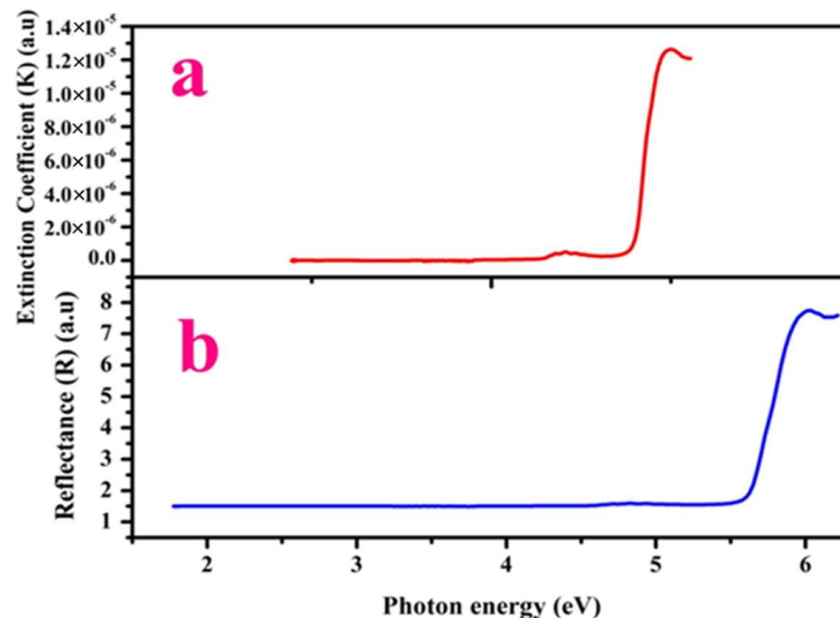


Figure 4. Cont.

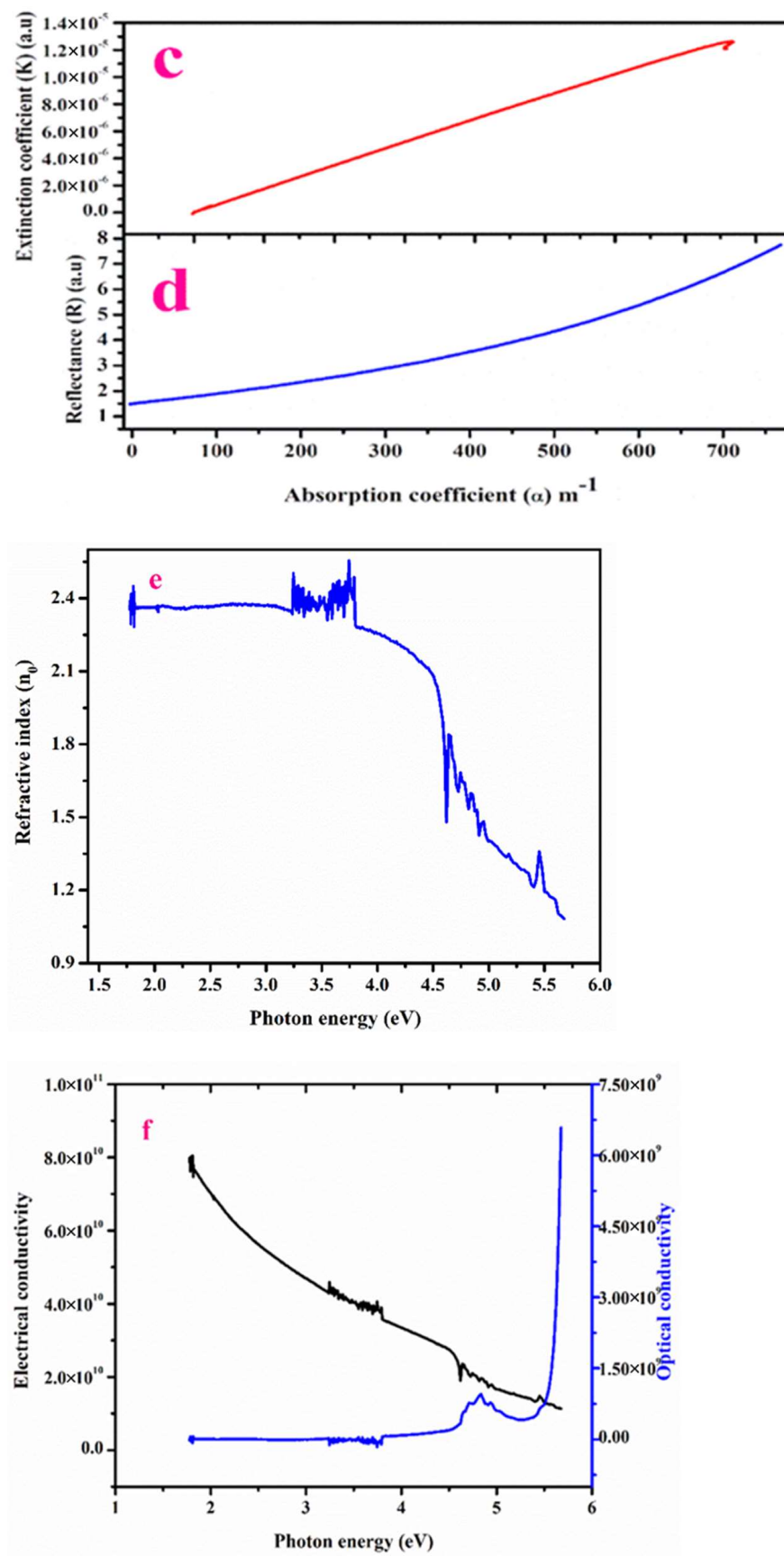


Figure 4. Cont.

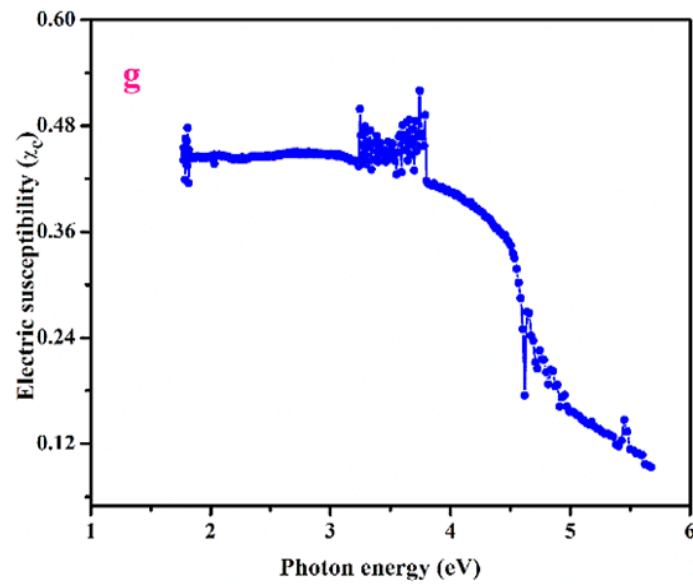


Figure 4. Variation of reflectance and extinction coefficient vs. (i) photon energy (a,b), (ii) absorption coefficient (α) (c,d). Plot of photon energy vs. (i) refractive index (n_0) (e). (ii) electrical conductivity and optical conductivity (f) (iii) Electric susceptibility (χ_c) (g).

The optical conductivity (σ_{op}) is,

$$\sigma_{op} = \frac{\alpha n_0 c}{4\pi} \quad (6)$$

and also the electrical conductivity (σ_{ele}) can be evaluated using the following formula,

$$\sigma_{ele} = \frac{2\lambda\sigma_{op}}{\alpha} \quad (7)$$

Figure 4e describes the elevation of optical conductivity with the increase in $h\nu$, for which a large value confirms the elevated photo-tunable feature of crystal [4]. Figure 4f concludes that the value of electrical and optical conductivity depends on the photon energy. Hence, this potential material is suitable in the ultrafast data transmission process (optical) [21].

The below relation depicts electric susceptibility (χ_c),

$$\epsilon_r = \epsilon_0 + 4\pi\chi_c = n_0^2 - K^2 \quad (8)$$

(Or)

$$\chi_c = \frac{n_0^2 - K^2 - \epsilon_0}{4\pi} \quad (9)$$

The electric susceptibility χ_c is 0.1314 for the wavelength 390 nm (Figure 4g).

The dielectric constants can be estimated using the following:

$$\epsilon = (n_0 + iK)^2 \quad (10)$$

$$\epsilon = n_0^2 - K^2 + 2in_0K = \epsilon_r + i\epsilon_i \quad (11)$$

$$\epsilon_r = n_0^2 - K^2 \text{ and } \epsilon_i = 2n_0K \quad (12)$$

At the wavelength of 390 nm, the real (ϵ_r) and imaginary (ϵ_i) parts were estimated as 1.6235 and 6.7139×10^{-7} . Hence, the low magnitude of the dielectric constant with a broad energy gap of the L-phenylalanine L-phenylalaninium malonate crystal suggests its fitness for optoelectronic devices.

3.3.2. Determination of Urbach Energy (E_u)

The dependence of α on $h\nu$ in the Urbach relation is [22],

$$\alpha(h\nu) = \alpha_0 \exp\left(\frac{h\nu}{E_u}\right) \quad (13)$$

The slope is 1.0817. Figure 5 illustrates the logarithm of (α) with the incident energy of the photon ($h\nu$). The inverse of the linear plot measures the Urbach energy (E_u), which was evaluated as 0.9244 eV. The lower calculated value of E_u indicates less flaws in LPPMA which validates its usage in nonlinear optics.

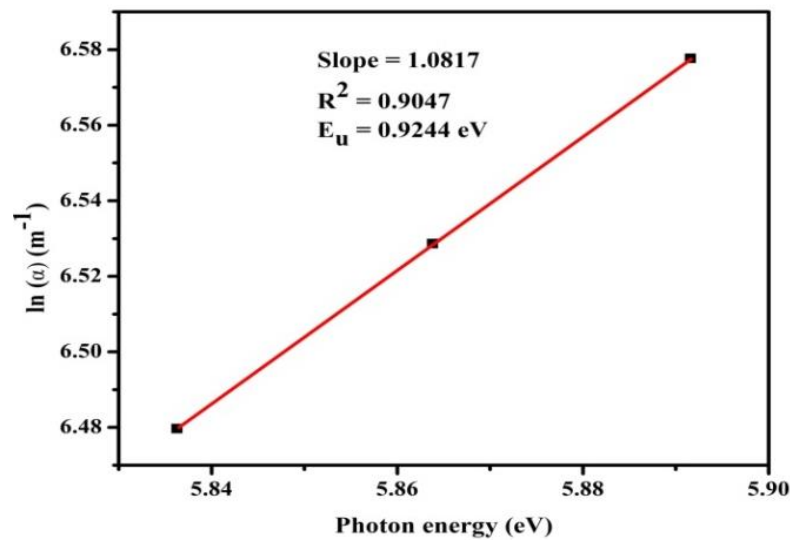


Figure 5. Plot $\ln(\alpha)$ vs. $h\nu$ for LPPMA.

3.4. Mechanical Stability Analysis

The hardness of the material determines its features, including its mechanical strength and its properties [23]. The mechanical stability of an optical crystal plays a key role in the fabrication of the device. The mechanical hardness of the LPPMA sample was tested utilizing an MH-112 Vickers hardness tester. The application of the load is (25 g, 50 g, 100 g) on the surface of LPPMA. The Vickers hardness number H_v of LPPMA was premeditated using the following expression (Table 2):

$$H_v = 1.8544 \frac{P}{d^2} \left(\text{kg/mm}^2 \right) \quad (14)$$

Table 2. Mechanical parameters of LPPMA.

Load P (g)	H_v (kg mm ⁻²)	H_k (kg mm ⁻²)	σ_y (GPa)	C_{11} (GPa)
25	8.76	0.067	11.99	68.99
50	13.30	0.102	18.19	104.66
100	19.15	0.147	26.19	150.71
200	25.5	0.196	34.88	200.72

The plot (Figure 6a) revealed that the elevation in H_v (hardness number) with load (25 g, 50 g, 75 g) emphasizes the reverse-indentation-size effect [23]. As can be observed from Figure 6b, the hardening coefficient is 3.71. Hence, the Meyer's index magnitude (n) infers that LPPMA possesses the feature of a soft nature.

The yield strength of LPPMA (Figure 6c) can be found using [24] Table 2,

$$\sigma_y = \frac{H_v}{3}(0.1)^{n'-2} \quad (15)$$

Here, the value of $n' = n + 2$.

The stiffness constant C_{11} is calculated using the following [25] Table 2 (Figure 6d):

$$\sigma_y = \frac{H_v}{3}(0.1)^{n'-2} \quad (16)$$

The Knoop hardness number (H_k) is determined by [24] Table 2,

$$H_k = 14.229 \frac{P}{d^2} \left(\text{kg/mm}^2 \right) \quad (17)$$

3.5. Determination of Dielectric Studies

The dielectric measurement provides details about the electrical response parameter of a periodic solid [26]. The dielectric constant and loss in LPPMA was performed across diverse temperature ranges using an LCR meter. This was calculated by:

$$\epsilon' = \frac{Ct}{A\epsilon_0} \quad (18)$$

and

$$\epsilon'' = \epsilon' \tan \delta \quad (19)$$

Here, C represents the capacitance specified by micro farad, t the thickness specified in mm, ϵ_0 is the dielectric constant in vacuum ($\epsilon_0 = 8.854 \times 10^{-12} \text{ Fm}^{-1}$) and A indicates the area of the testing material in mm^2 . Figure 7a,b shows variations of ϵ' and ϵ'' with log frequency and it reduces with a rise in frequency. The higher values of ϵ' at smaller frequencies is a result of all polarization mechanisms. The lower range of (ϵ') at the domain of a higher range of frequency may possibly originate with respect to the electric field applied [26]. The lower measure of ϵ' and ϵ'' at a high frequency range indicates the enhanced optical nature with the minimal amount of defects in LPPMA, which furthermore fulfills the requirements for use in the opto-electronic sector and in nonlinear optical devices [26].

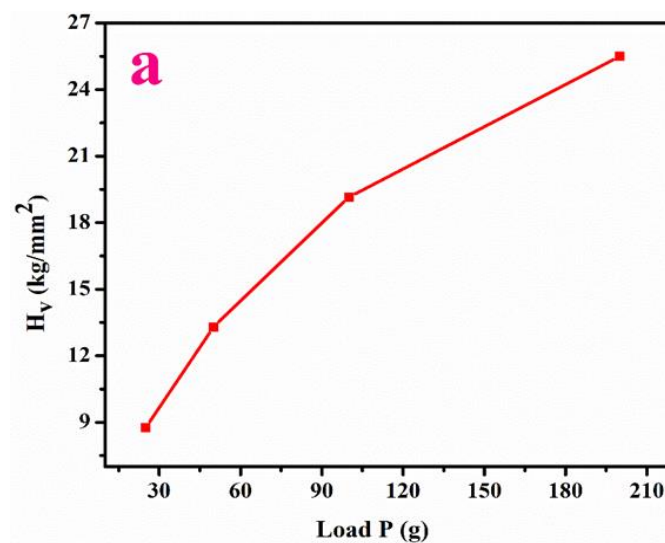


Figure 6. Cont.

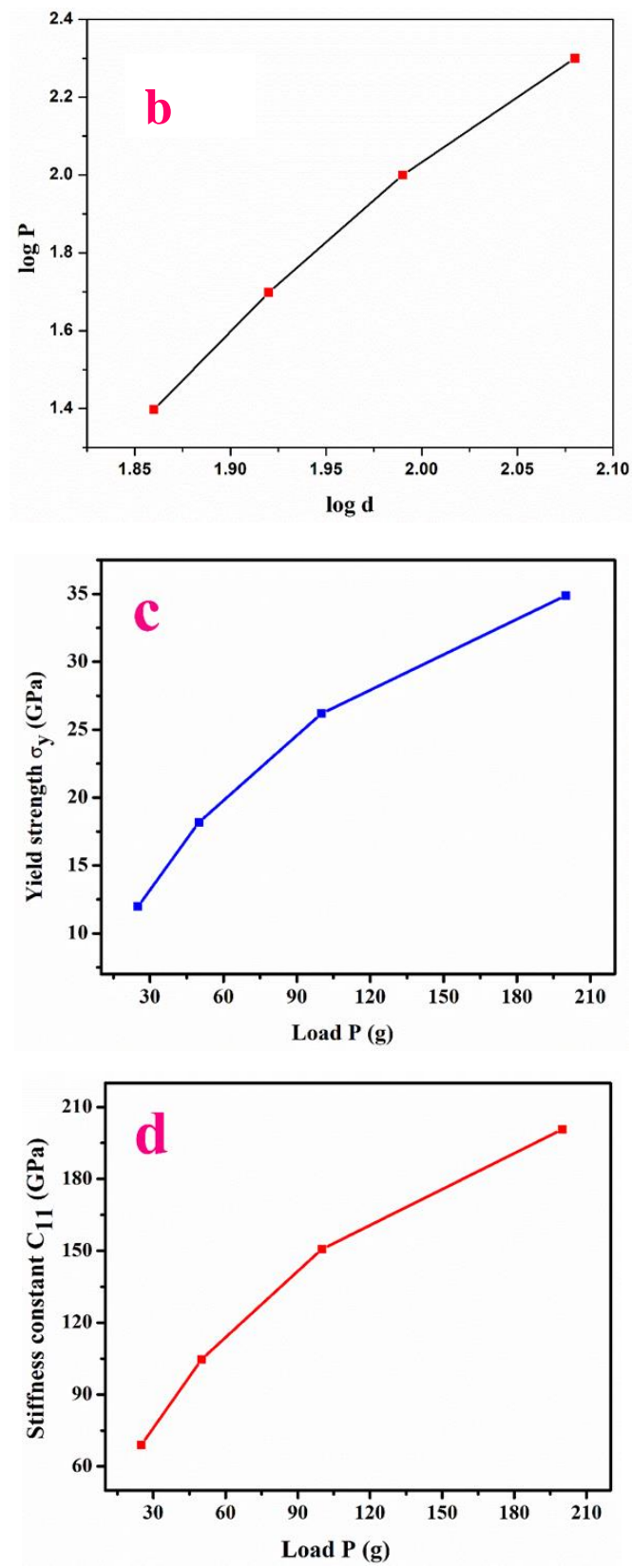


Figure 6. Cont.

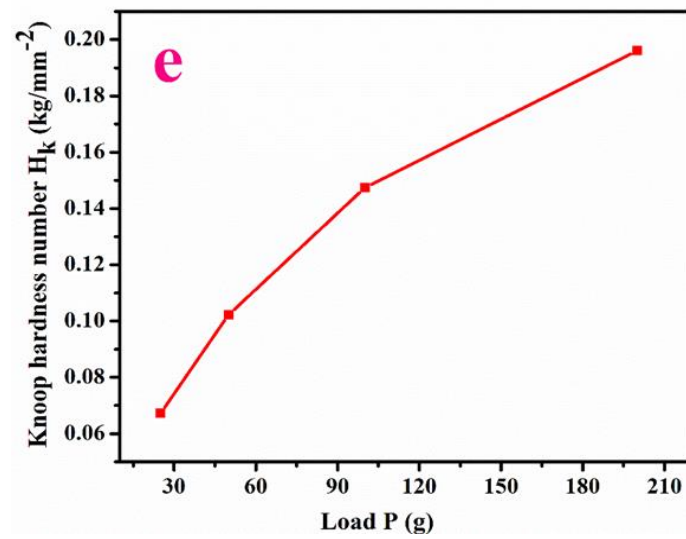


Figure 6. (a–e) Hardness value, Meyers graph, Yield strength, Stiffness constant, Knoop hardness.

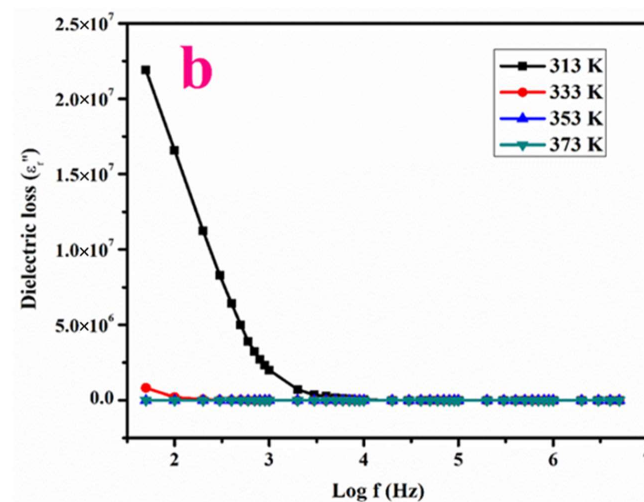
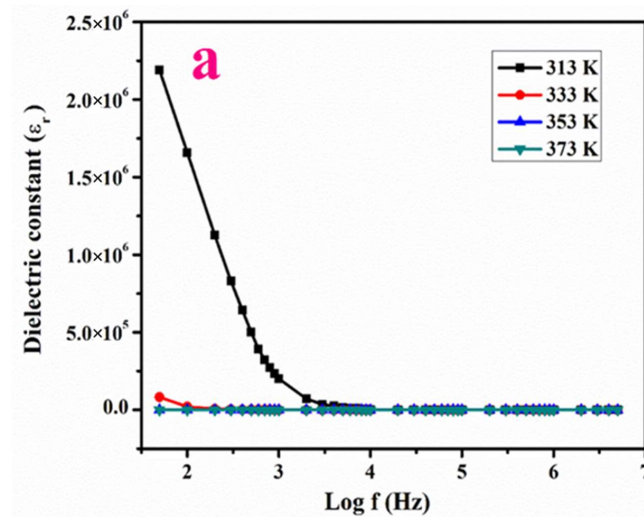


Figure 7. Cont.

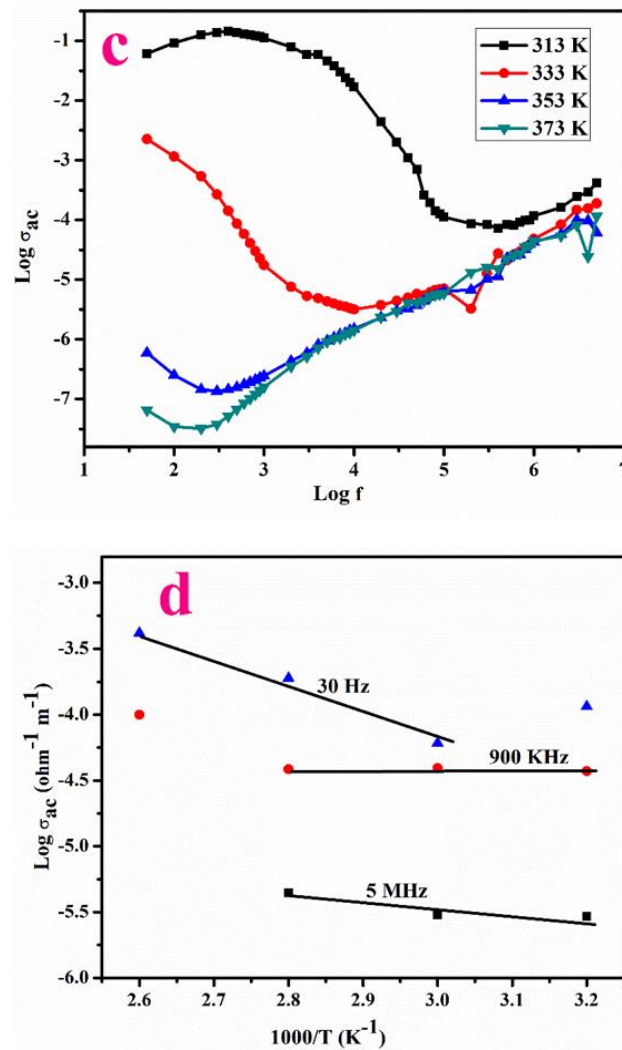


Figure 7. Variation of (a,b) logarithm of frequency versus dielectric constant, dielectric loss, (c,d) Logarithm of ac conductivity versus log f.

The ac conductivity σ_{ac} ($\Omega \text{ m}$)⁻¹ was evaluated using the following relation (23):

$$\sigma_{ac} = 2\pi f \epsilon_0 \epsilon' \tan \delta \tag{20}$$

The variation of conductivity with log ω at diverse temperatures is depicted in Figure 7c.

Energy of Activation

E_a (activation energy) estimated using the formula,

$$\sigma = \sigma_0 \exp\left(-\frac{E_a}{k_B T}\right) \tag{21}$$

where σ_{ac} represents conductivity and k_B signifies the Boltzmann constant. Figure 7d displays the relation of logarithm of ac conductivity with $1000/T$ which is found to be nearly linear in nature and E_a is evaluated using the following expression,

$$E_a = -\text{slope} * 1000 * k_B \tag{22}$$

The E_a values are 0.3733, 0.055 and 0.093 eV at the frequency of 30 KHz, 900 KHz and 5 MHz. Its lower value indicates that the LPPMA contains a lower number of defects, which is suitable for device fabrication [23].

3.6. Fluorescence Analysis

The luminescence spectrum of LPPMA was measured to emphasize its emission nature and its spectra are presented in Figure 8a, using a wavelength of excitation of 233 nm. The highest peak in emission occurred at 535 nm (2.31 eV), in the visible range spectrum. The peaks at 454 nm (2.73 eV) and 511 nm (2.42 eV) were attributed to defects existing in the material.

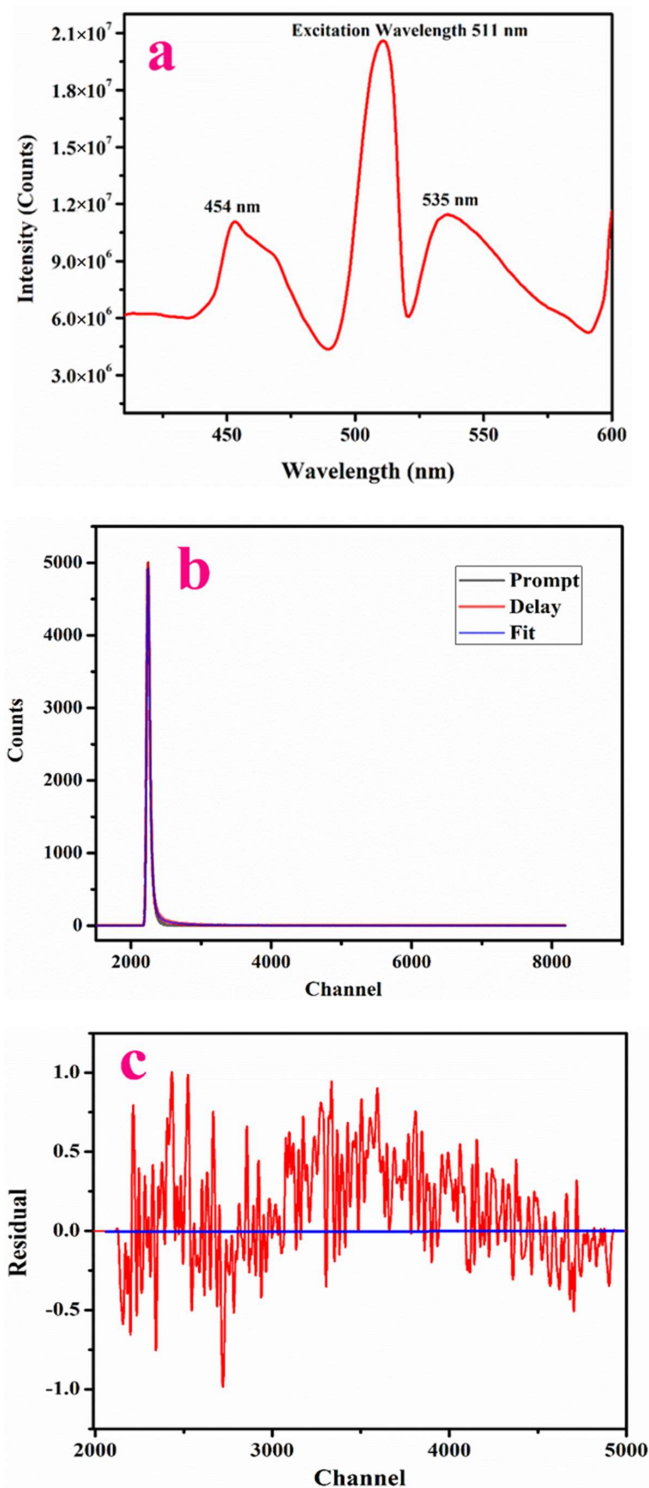


Figure 8. (a) Emission spectra of LPPMA; (b) Fluorescence life time spectra of LPPMA, (c) Residual Fit of LPPMA.

3.7. NLO Characterization

The proficiency of SHG was established using Kurtz' and Perry's analysis [27,28] in comparison with KH_2PO_4 (KDP). Here, LPPMA was illuminated using a Neodymium:YAG laser (1064 nm) with a specified pulse width (10 ns). The conversion efficiency in SHG of LPPMA was 0.38 times that of KH_2PO_4 .

3.8. Z-Scan Measurements

The third-order acentric nonlinearities likely have a nonlinear refractive index (n_2) nonlinear absorption coefficient (β) and III-order optical susceptibility ($\chi^{(3)}$), which were assessed using the Z-scan method [29]. β and n_0 values were measured by the closed and open aperture Z-scan method.

The difference in transmittance (peak and valley) (ΔT_{P-V}) along with on-axis phase shift $|\Delta\Phi_0|$ is,

$$\Delta T_{P-V} = 0.406(1 - S)^{0.25} |\Delta\Phi_0| \quad (23)$$

$$S = 1 - \exp\left(\frac{-2r_a^2}{\omega_a^2}\right) \quad (24)$$

Here, S and r_a , denote aperture transmittance and aperture radius.

The third-order nonlinear refractive index is [21],

$$n_2 = \frac{\Delta\Phi_0}{KI_0L_{\text{eff}}} \quad (25)$$

The imaginary portion ($\chi^{(3)}$) is calculated by β (nonlinear absorption), which is obtained using the following formula,

$$\beta = \frac{2\sqrt{2}\Delta T}{I_0L_{\text{eff}}} \quad (26)$$

$$\text{Re}\chi^{(3)}(\text{esu}) = \frac{10^{-4}(\epsilon_0 C^2 n_0^2 n_2)}{\pi} \left(\frac{\text{cm}^2}{\text{W}}\right) \quad (27)$$

$$\text{Im}\chi^{(3)}(\text{esu}) = \frac{10^{-2}(\epsilon_0 C^2 n_0 \lambda \beta)}{4\pi^2} \left(\frac{\text{cm}^2}{\text{W}}\right) \quad (28)$$

$$|\chi^{(3)}| = \sqrt{(\text{Re}(\chi^{(3)}))^2 + (\text{Im}(\chi^{(3)}))^2} \quad (29)$$

The closed aperture plot for LPPMA is specified in Figure 9a. The peak followed by a valley in the curve (normalized transmittance) is a sign of negative non-linearity and the self-defocusing effect [29,30] which makes it a suitable candidate in the optical sensor domain [31]. The curve in open aperture is presented in Figure 9b. The magnitude of β is premeditated, which shows a positive measure that indicates the absorption processes [21]. The materials that demonstrate two photon practices are broadly applied in light-based power limiting uses [32–35]. The calculated data of Z-scan visibly specify that LPPMA displays excellent third-order acentric characteristics, which are presented in Table 3. The value of $\chi^{(3)}$ has a higher magnitude in comparison to other NLO materials in Table 4. Thus, the excellent NLO characteristics of LPPMA prove it to be suited to optical limiting applications.

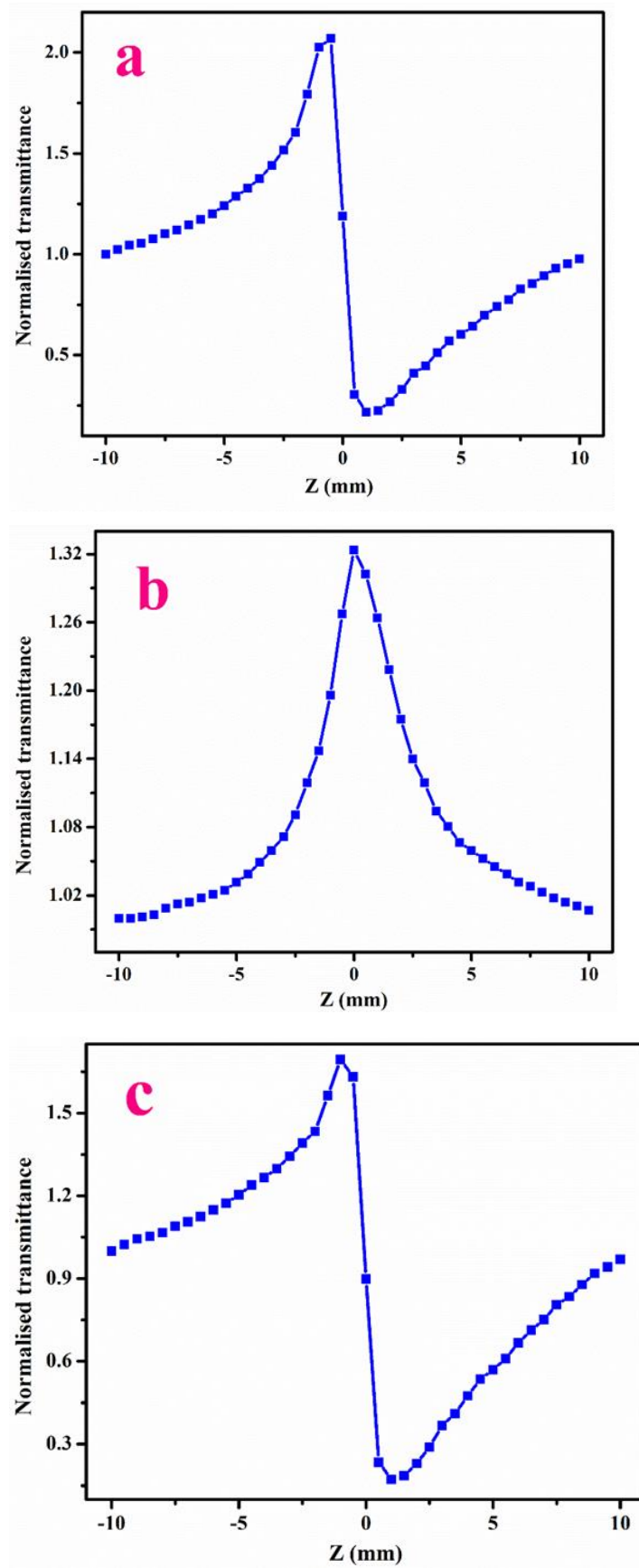


Figure 9. (a) Closed aperture and (b) Open aperture (c) Ratio of the closed-to-open Z-scan traces of LPPMA.

Table 3. Nonlinear optical parameters for LPPMA.

Parameters	Measured Values for LPPMA
(n_2) —Nonlinear refractive index	$7.06 \times 10^{-8} \text{ cm}^2\text{W}^{-1}$
(β) —Nonlinear absorption coefficient	$0.21 \times 10^{-4} \text{ cmW}^{-1}$
$[\text{Re}(\chi^3)]$ —Real part of susceptibility	$2.90 \times 10^{-6} \text{ esu}$
$[\text{Im}(\chi^3)]$ —Imaginary part of susceptibility	$1.31 \times 10^{-6} \text{ esu}$
(χ^3) —Third-order NLO susceptibility	$3.19 \times 10^{-6} \text{ esu}$

Table 4. $\chi^{(3)}$ values of LPPMA comparison with new NLO materials.

Crystal	Third-Order Susceptibility $\chi^{(3)}$	Reference
LPPMA	$3.19 \times 10^{-6} \text{ esu}$	Present Work
LMSA	$6.34 \times 10^{-6} \text{ esu}$	[32]
LAPA	$5.24 \times 10^{-7} \text{ esu}$	[33]
VMST	$9.69 \times 10^{-12} \text{ esu}$	[34]

4. Conclusions

LPPMA were efficiently produced using a slow evaporation process with water as the solvent at a constant temperature. The lattice parameters were estimated using single-crystal XRD. The existence of functional groups in the material was established with an FTIR analysis. The UV-visible spectrum study revealed good transmittance in the area of the visible spectrum, which indicates a cut-off wavelength at 233 nm and energy-gap value of 5.53 eV from which various optical parameters were evaluated to analyze its suitability in optical processing. LPPMA belongs to the soft material group which was identified during the hardness analysis. The dielectric studies prove the presence of a flawless material. The second harmonic generation was observed through the Kurtz Perry procedure, which revealed SHG efficiency of 0.38 times that of KDP. The third order acentric parameters were estimated and attest to its reliable usage in future photonics applications.

Author Contributions: P.S. and M.N. experimental design and write first draft, C.R.T.K. and S.S. and G.V. did data validation and analysis while G.M. and A.M. did supervision. M.L.C., A.K. formal analysis and conceptualization, H.S.A., M.A.H. and M.P. write final draft of the manuscript. All authors have read and agreed to the published version of the manuscript.

Funding: The Deanship of Scientific Research (DSR), King Abdulaziz University, Jeddah Saudi Arabia has funded this project, under grant No. (KEP-35-130-42).

Institutional Review Board Statement: Not applicable.

Informed Consent Statement: Not applicable.

Data Availability Statement: Not applicable.

Conflicts of Interest: The authors declare no conflict of interest.

References

1. Caroline, M.L.; Sankar, R.; Indirani, R.; Vasudevan, S. Growth, optical, thermal and dielectric studies of an amino acid organic nonlinear optical material: L-Alanine. *Mater. Chem. Phys.* **2009**, *114*, 490–494. [[CrossRef](#)]
2. Selvakumar, E.; Chandramohan, A.; Babu, G.A.; Ramasamy, P. Synthesis, growth, structural, optical and thermal properties of a new organic salt crystal: 3-nitroanilinium trichloroacetate. *J. Cryst. Growth* **2014**, *401*, 323–326. [[CrossRef](#)]
3. Caroline, M.L.; Vasudevan, S. Growth and characterization of L-phenylalanine nitric acid, a new organic nonlinear optical material. *Mater. Lett.* **2009**, *63*, 41–44. [[CrossRef](#)]
4. Jayaprakash, P.; Sangeetha, P.; Kumari, C.R.; Caroline, M.L. Investigation on the growth, spectral, lifetime, mechanical analysis and third-order nonlinear optical studies of L-methionine admixed DL mandelic acid single crystal: A promising material for nonlinear optical applications. *Phys. B Condens. Matter* **2017**, *518*, 1–12. [[CrossRef](#)]

5. Suresh, S. The growth and the optical, mechanical, dielectric and photoconductivity properties of a new nonlinear optical crystal-L-phenylalanine 4-nitrophenol NLO single crystal. *J. Cryst. Process Technol.* **2013**, *3*, 87–91. [[CrossRef](#)]
6. Jayaprakash, P.; Mohamed, M.P.; Krishnan, P.; Nageshwari, M.; Mani, G.; Caroline, M.L. Growth, spectral, thermal, laser damage threshold, microhardness, dielectric, linear and nonlinear optical properties of an organic single crystal: L-phenylalanine DL-mandelic acid. *Phys. B Condens. Matter* **2016**, *503*, 25–31. [[CrossRef](#)]
7. Ahmadivand, A.; Gerislioglu, B. Deep and vacuum-ultraviolet metaphotonic light sources. *Mater. Today* **2021**, *51*, 208–221. [[CrossRef](#)]
8. Jayaprakash, P.; Sangeetha, P.; Mohamed, M.P.; Vinitha, G.; Muthu, S.; Prakash, M.; Caroline, M.L. Growth and characterization of DL-Mandelic acid (C₆H₅CH(OH)CO₂H) single crystal for third-order nonlinear optical applications. *J. Mol. Struct.* **2017**, *1148*, 314–321. [[CrossRef](#)]
9. Prakash, M.; Geetha, D.; Caroline, M.L. Growth and characterization of nonlinear optical (NLO) active L-phenylalanine fumaric acid (LPFA) single crystal, Materials and manufacturing process. *Mater. Manuf. Process.* **2012**, *27*, 519–522. [[CrossRef](#)]
10. Prakash, M.; Geetha, D.; Caroline, M.L. Crystal growth and characterization of L-phenylalaninium trichloroacetate—A new organic nonlinear optical material. *Phys. B Condens. Matter* **2011**, *406*, 2621–2625. [[CrossRef](#)]
11. Prakash, M.; Caroline, M.L.; Geetha, D. Growth, structural, spectral, optical and thermal studies on amino acid based new NLO single crystal: L-phenylalanine- 4-nitrophenol. *Spect. Acta Part A Mol. Biomol. Spect.* **2013**, *108*, 32–37. [[CrossRef](#)] [[PubMed](#)]
12. Prakash, M.; Geetha, D.; Caroline, M.L. Synthesis, structural, optical, thermal and dielectric studies on new organic nonlinear optical crystal by solution growth technique. *Spect. Acta Part A Mol. Biomol. Spect.* **2013**, *107*, 16–23. [[CrossRef](#)] [[PubMed](#)]
13. Sangeetha, P.; Jayaprakash, P.; Nageshwari, M.; Kumari, C.R.; Sudha, S.; Prakash, M.; Vinitha, G.; Caroline, M.L. Growth and characterization of an efficient new NLO single crystal L-phenylalanine D-methionine for frequency conversion and optoelectronic applications. *Phys. B Condens. Matter* **2017**, *525*, 164–174. [[CrossRef](#)]
14. Beaujon, J.H.; Straughn Jr, W.R.; Hartung, W.H. Amino acids. XII. Preliminary nutritional and enzymatic studies of malonic acid analogs of natural alpha-amino acids. *J. Am. Pharm. Assoc.* **1952**, *41*, 581. [[CrossRef](#)] [[PubMed](#)]
15. de Villepin, J.; Limage, M.-H.; Novak, A.; Toupry, N.; Le Postollec, M.; Poulet, H.; Ganguly, S.; Rao, C.N.R. Raman study of high-temperature phase transition of malonic acid. *J. Ram. Spect.* **1984**, *15*, 1. [[CrossRef](#)]
16. Blanchet, J.; Baudoux, J.; Amere, M.; Lasne, M.C.; Rouden, J. Asymmetric malonic and acetoacetic acid synthesis, A century of enantioselective decarboxylative protonations. *Eur. J. Org. Chem.* **2008**, *33*, 5493–5506. [[CrossRef](#)]
17. Alagar, M.; Krishnakumar, V.; Devi, P.P.; Natarajan, S. L-phenylalanine L-phenylalaninium malonate. *Acta Crystallogr. Sect. E Struct. Rep. Online* **2005**, *61*, 7014. [[CrossRef](#)]
18. Prakash, M.; Geetha, D.; Caroline, M.L.; Ramesh, P. Crystal growth, structural, optical, dielectric and thermal studies of an amino acid based organic NLO material: L-phenylalanine L-phenylalaninium malonate. *Spectrochim. Acta Part A Mol. Biomol. Spectrosc.* **2011**, *83*, 461–466. [[CrossRef](#)]
19. Srinivasan, P.; Vidyalakshmi, Y.; Gopalakrishnan, R. Studies and synthesis, growth and crystal structure and nonlinear optical properties of a novel nonlinear optical crystal: L-Argininium 4 nitro Phenolate Monohydrate (LARP). *Cryst. Grow. Des.* **2008**, *8*, 2329–2334. [[CrossRef](#)]
20. Socrates, G. *Infrared and Raman Characteristic Group Frequencies*, 3rd ed.; John Wiley & Sons Publishers: Hoboken, NJ, USA, 2001.
21. Jayaprakash, P.; Sangeetha, P.; Kumari, C.R.T.; Baskaran, I.; Caroline, M.L. Growth and characterization of L-asparagine monohydrate admixed DL mandelic acid nonlinear optical single crystal. *J. Mater. Sci. Mater. Electron.* **2017**, *28*, 18787–18794. [[CrossRef](#)]
22. Kumari, C.R.T.; Nageshwari, M.; Jayaprakash, P.; Sangeetha, P.; Sudha, S.; Caroline, M.L. Investigation on growth, optical, thermal, mechanical, dielectric, LDT studies of sulphanic acid monohydrate: A promising third-order nonlinear optical material. *J. Nonlinear Opt. Phys. Mater.* **2017**, *26*, 1750020. [[CrossRef](#)]
23. Jayaprakash, P.; Mohamed, M.P.; Caroline, M.L. Growth, spectral and optical characterization of a novel nonlinear optical organic material: D-Alanine DL-mandelic acid single crystal. *J. Mol. Struct.* **2017**, *1134*, 67–77. [[CrossRef](#)]
24. Nageshwari, M.; Jayaprakash, P.; Kumari, C.R.T.; Vinitha, G.; Caroline, M.L. Growth, spectra, linear and nonlinear optical characteristics of an efficient semiorganic acentric crystal: L-valinium L-valine chloride. *Phys. B Condens. Matter* **2017**, *511*, 1–9. [[CrossRef](#)]
25. Surekha, R.; Gunaseelan, R.; Sagayaraj, P.; Ambujam, K. L-phenylalanine L-phenylalaninium bromide—a new nonlinear optical material. *CrystEngComm* **2014**, *16*, 7979–7989. [[CrossRef](#)]
26. Senthil, K.; Kalainathan, S.; Kumar, A.R.; Aravindan, P.G. Investigation of synthesis, crystal structure and third-order NLO properties of a new stilbazolium derivative crystal: A promising material for nonlinear optical devices. *RSC Adv.* **2014**, *4*, 56112–56127. [[CrossRef](#)]
27. Sangeetha, P.; Jayaprakash, P.; Ramesh, P.; Sudha, S.; Vinitha, G.; Nageshwari, M.; Caroline, M.L. Crystal growth, spectroscopic, optical, thermal and hirshfeld surface analysis of glyciniun hydrogen fumarate glycine solvate monohydrate (GHFGSM): A third harmonic nonlinear optical organic crystal. *J. Mol. Struct.* **2020**, *1213*, 128187. [[CrossRef](#)]
28. Kurtz, S.K.; Perry, T.T. A powder technique for the evaluation of nonlinear optical materials. *J. Appl. Phys.* **1968**, *39*, 3798–3813. [[CrossRef](#)]

29. Vivek, P.; Suvitha, A.; Murugakoothan, P. Growth, spectral, anisotropic, second and third order nonlinear optical studies on potential nonlinear optical crystal anilinium perchlorate (AP) for NLO device fabrication. *Spectrochim. Acta Part A Mol. Biomol. Spectrosc.* **2015**, *134*, 517–525. [[CrossRef](#)]
30. Shettigar, S.; Umesh, G.; Chandrasekharan, K.; Kalluraya, B. Third order nonlinear optical properties and two photon absorption in newly synthesized phenyl sydnone doped polymer. *Synth. Met.* **2007**, *157*, 142–146. [[CrossRef](#)]
31. Wei, Y.-Z.; Sridhar, S. A new graphical representation for dielectric data. *J. Chem. Phys.* **1993**, *99*, 3119–3124. [[CrossRef](#)]
32. Sangeetha, P.; Jayaprakash, P.; Nageshwari, M.; Mohamed, M.P.; Vinitha, G.; Caroline, M.L. Growth and characterization of L-phenylalanine nitric acid (LPN) and Tris L-(phenylalanine)-phenylalaninium nitrate (TPLPN) as second and third order nonlinear optical materials. *Chin. J. Phys.* **2018**, *56*, 721–739. [[CrossRef](#)]
33. Nageshwari, M.; Kumari, C.R.; Vinitha, G.; Mohamed, M.P.; Sudha, S.; Caroline, M.L. Crystal growth, structural, spectral, thermal, dielectric, linear and nonlinear optical characteristics of a new organic acentric material: L-Methionine-Succinic acid (2/1). *J. Mol. Struct.* **2018**, *1155*, 101–109. [[CrossRef](#)]
34. Mani, R.J.; Selvarajan, P.; Devadoss, H.A.; Shanthi, D. Second-order and third-order NLO and other properties of L-alanine crystal admixture with perchloric acid (LAPA). *Optik* **2014**, *126*, 213. [[CrossRef](#)]
35. Kumar, M.K.; Sudhakar, S.; Pandi, P.; Bhagavannarayana, G.; Kumar, R.M. Studies of the structural and third-order nonlinear optical properties of solution grown 4-hydroxy-3-methoxy-4-N-methylstibazoliumtosylate monohydrate crystals. *Opt. Mater.* **2014**, *36*, 988. [[CrossRef](#)]